COMPRESSIVE CREEP BEHAVIOR OF ZIRCONIA/NICKEL OXIDE COMPOSITES

F.A. Huamán-Mamani[1] and M. Jiménez-Melendo[2]

[1] Universidad Católica San Pablo, Quinta Vivanco s/n, Urb. Campiña Paisajista, Arequipa, Peru (fhuaman@ucsp.edu.pe)
[2] Universidad de Sevilla, Departamento de Física de la Materia Condensada, 41012 Sevilla, Spain (melendo@us.es)

Keywords: Creep, Zirconia, Nickel oxide, Ceramic composites

ABSTRACT

Nickel oxide/zirconia composites with different NiO contensts have been fabricated by mechanical mixing of nickel oxide and zirconia powders and sintering at 1500 ºC for 10 h in air. The resulting microstructures have been characterized by scanning and transmission electron microscopy. The mechanical behaviour of the composites has been characterized by compressive tests at high temperatures between 1100 and 1350 ºC. For NiO contents above the percolation limit, the softer phase was found to be rate-controlling in oxidizing atmospheres, achieving extended steady states of deformation without macroscopic failure. By contrast, the overall creep strength of the composites decreased severely in reducing conditions.

1 INTRODUCTION

Ceramic-metal composites (cermets) based on zirconia and nickel have been intensively studied in the last years because their conducting properties can be easily tailored for particular applications as sensors, thermal barriers and particularly as anodes for solid state fuel cells (SOFCs) [1-2]. These devices operate at relatively high temperatures and are very efficient in the electrochemical conversion of different fuels (hydrogen, natural gas, …) into electricity. Zirconia/nickel cermets are usually produced using nickel oxide as precursor powder. This compound is then reduced to metallic nickel during the first use of the fuel cell at high temperatures. This procedure give rises to significant changes in the morphology and microstructure of the composite, which may decrease the electrochemical efficiency of the device since it is directly related to the microstructural characteristics of the nickel and zirconia phases in the cermet [3,4]. Furthermore, creep and deformation processes take place during SOFC operation at elevated temperatures, which may affect negatively the integrity of the composite and compromise in turn the overall performance of the device, in particular under reducing atmospheres.

In this work, we have investigated the high-temperature mechanical response of nickel oxide/zirconia composites under different atmospheres in compression. Firstly, composites with different NiO contents were fabricated by conventional ceramic routes. After microstructural characterization, the composites were submitted to mechanical tests at high temperatures in compression. Similar tests were performed on monolithic NiO and zirconia counterparts for the sake of comparison.

2 EXPERIMENTAL PROCEDURE

2.1. Material.

Composites with NiO contents of 40 and 65 mol% were obtained starting from a mixture of commercial powders of nickel oxide (99.8 wt.% purity, average particle size < 50 nm, Sigma Aldrich) and zirconia. Two types of zirconia powders were used: 8 mol% Y_2O_3-fully stabilized cubic ZrO_2 (8YSZ, impurity content < 0.03 wt.%, average crystallite size of 25 nm, 8YSZ grade, Tosoh Corp., Japan) and 3 mol% Y_2O_3-stabilized tetragonal ZrO_2 (impurity content < 0.26 wt.%, average crystallite size of 26 nm, TZ-3Y-E grade, Tosho Corp., Japan). Appropriate amounts of the powders were first

ball-milled in agate media for 1 h and then uniaxially compressed at 150 MPa into 20 mm diameter pellets, followed by cold isostatic pressing at 210 MPa. These pellets were then sintered at 1500 ºC for 10 h in air atmosphere. Monolithic zirconia and monolithic nickel oxide were also processed for the sake of comparison following the same fabrication schedule. Bulk densities were measured from weight/dimensions measurements of the samples. Theoretical densities were calculated from the rule of mixtures by taking 5900, 6080 and 6670 kg/m^3 for the densities of cubic 8YSZ, tetragonal 3YTZP and NiO, respectively.

2.2. Microstructural characterization

Specimen microstructures were analyzed by scanning (SEM) and transmission (TEM) electron microscopy (Microscopy Service, CITIUS, University of Seville, Spain). For SEM observations, sections were cut from the as-received materials and then metallographycally polished with water-cooled SiC papers, finishing with 1-μm grade diamond paste. In order to reveal the grain boundaries, these sections were thermally etched at 1300 ºC for 2 h. The relevant morphological parameters measured for the different materials using a semiautomatic image analyzer were: the grain size d (taken as the equivalent planar diameter), the form factor F and the orientation angle W (defined as the angle formed by the largest diameter of the grains relative to a fixed direction, i.e., the angle of the maximum Feret's diameter). TEM specimens were prepared following conventional techniques of mechanical grinding, dimpling and ion-milling of sliced sections.

2.3. Mechanical tests

For mechanical testing, rectangular prismatic samples of about 5 x 3 x 3 mm were cut from the sintered compounds. Compressive tests were performed at temperatures between 1100 and 1300 ºC under different environments (air, inert and reducing atmospheres) at constant cross-head speeds between 5 and 100 μm, corresponding to initial strain rates of $2x10^{-5}$ and $4x10^{-4}$ s^{-1}, respectively. The recorded data, load vs time, were analysed in σ - ε curves, where σ is the true stress and ε is the true strain (= $\ln(l_o/l)$, with l_o and l the initial and instantaneous length, respectively). The specimens were plastically deformed to typical total strains of about 50% for subsequent microstructural observations, unless premature failure occurred. Mechanical data were analyzed using the standard high-temperature power law for steady-state deformation [5]:

$$\dot{\varepsilon} = A\sigma^n \exp(-Q/RT) \quad (1)$$

where $\dot{\varepsilon}$ (= dε/dt) is the strain rate, A is a parameter depending on the deformation mechanism, n the stress exponent, Q the activation energy for flow and R the gas constant.

After mechanical testing, the microstructure of the strained samples was again investigated by SEM and TEM using the same procedures described above, looking for possible modifications in grain features and dislocations structures with respect to the as-received specimens.

3 RESULTS AND DISCUSSION

Fig. 1 shows representative SEM micrographs of the as-fabricated monolithic materials NiO, 3YTZP and 8YSZ, as well as of the composites. NiO exhibits a homogeneous and equiaxed grain size distribution (Fig. 1(a)), with average values of the form factor and grain size of 0.8 and 7.0 μm, respectively. Large pores of several μm in diameter can be observed at grain junctions. The relative bulk density is 90%, in agreement with SEM observations. On the other hand, cubic zirconia shows a similar microstructure (Fig. 1(b)) formed by equiaxed grains with a form factor of 0.8 and an average size of 5.5 μm, with very fine pores located mainly at triple grain junctions. These observations are consistent with the bulk density of 99.5% determined from weight/dimensions measurements. By contrast, monolithic 3YTZP exhibits a very homogeneous grain distribution (Fig. 1c)), with equiaxed grains of F = 0.8 and very fine sizes of d = 0.4 μm, as usually reported for this ceramic [6,7]; the relative density is 100%. The grain size distributions of these monoliths follow a lognormal law, as

found systematically in many ceramic materials and other physical systems [8].

Figs. 1(d)-(f) show typical SEM images of 8YSZ/NiO and 3YTZP/NiO composites. As expected from the characteristics of the parent phases, the composites exhibit duplex microstructures formed by zirconia and nickel oxide grains, without any third phase. It should be noted that the size of the zirconia grains in the composites remains similar to that found in the monoliths, while the average size of the NiO grains is reduced to half the value found in the monolith.

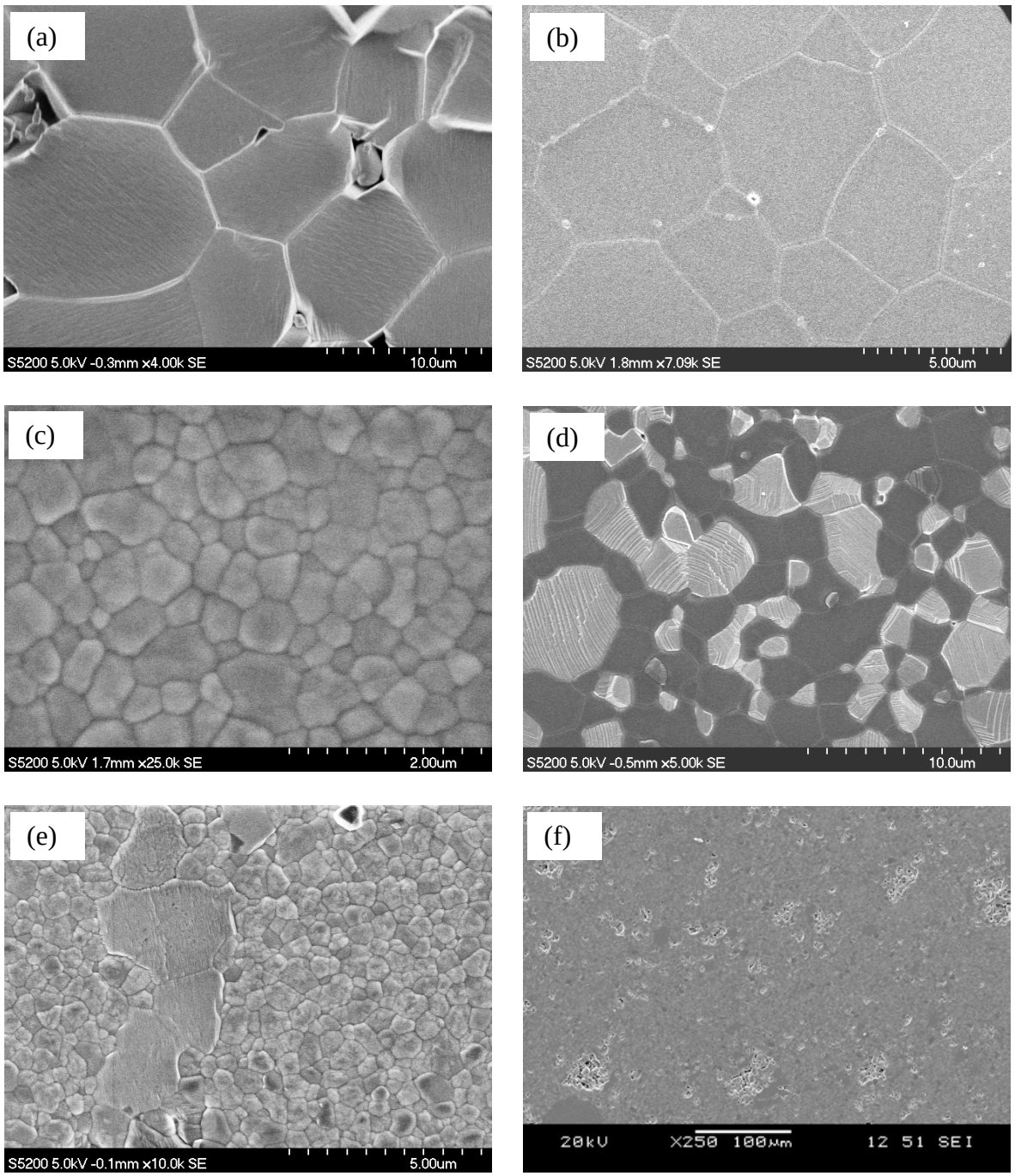

Figure 1: SEM micrographs showing the microstructure of: (a) monolithic NiO; (b) monolithic 8YSZ; (c) monolithic 3YTZ; (d) 65 mol NiO/8YSZ composite (dark phase: cubic zirconia, bright phase: nickel oxide); (e) 40 mol% NiO/3YTZP composite (small grains: tetragonal zirconia, large grains: nickel oxide); and (f) low-magnification micrograph of 65 mol NiO/8YSZ composite showing the inhomogeneous pore distribution.

Regarding the composite densities, they lie in between those of the monolithic counterparts; the overall density increases with decreasing NiO content. For example, values of 93% and 97% have been estimated for 40 mol% NiO/8YSZ and 40 mol% NiO/3YTZP composites, respectively. Porosity is not homogeneously distributed throughout the composites but is associated to the nickel oxide particles, with pore sizes of several μm (Fig. 2(f)).

Before studying the mechanical properties at elevated temperatures of the composites themselves, it is necessary to know the response of the monolithic constituents. Many studies have been devoted to study the plastic behavior of 8YSZ and 3YTP ceramics [6,7,9]. In fact, tetragonal zirconia is probably the most investigated of all ceramic materials in the last years because of its excellent mechanical properties: at low temperatures, the martensitic tetragonal-to-monoclinic transformation imparts fracture toughness and strength for structural applications; and at elevated temperatures, 3YTZP exhibits structural superplasticity due to the submicrometer grain size, which is indeed very stable against coarsening. Except at very low stresses (far from the present working conditions), the steady state of deformation is characterized by a stress exponent n of 1 (diffusional creep) in 8YSZ and 2 (grain boundary sliding) in 3YTZP [6,9], the difference being due to the large difference in grain size. In both materials, however, the activation energy for flow Q is about 500 kJ/mol, indicating that the strain rate is controlled by the same ionic species in both cubic and tetragonal zirconia.

On the contrary, experimental data for NiO are very scarce in the literature [10,11]. Fig. 2 shows true stress σ – true strain ε curves for monolithic NiO deformed at various initial strain rates and temperatures. After an initial peak stress, extended steady states of deformation were achieved, characterized by a rather constant slope in the σ – ε plot. As expected, the flow stress increases with decreasing temperature and increasing strain rate. The initial peak stress occurs by dislocation multiplication and blocking at glide planes (hardening), followed by a very fast dislocation annihilation once a cell structure is formed (softening). Finally, a steady state of deformation is achieved, corresponding to a dislocation recovery-controlled creep [5,10].

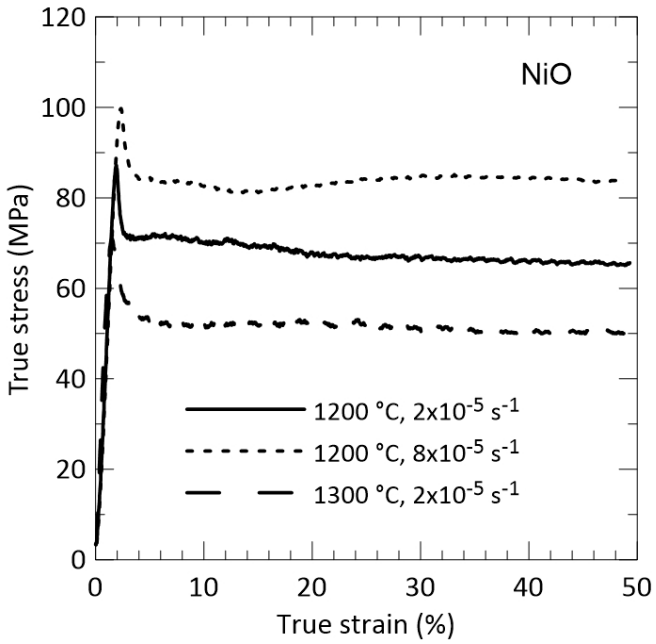

Figure 2: True stress against true strain curves at different temperatures and initial strain rates for NiO monoliths.

The stress exponent n and the activation energy for creep Q (eq. (1)) have been estimated from Fig. 2, resulting n = 9 and Q = 490 kJ/mol. This very high n value was previously reported for NiO single crystals and large-grained polycrystals [10,11], where the mechanism of recovery was ascribed to diffusion-controlled climb of dislocations. The Q value is also close to that reported in previous studies, 510 ± 60 kJ/mol, in which oxygen lattice diffusion was found to be the rate-controlling species

[10].

Regarding the mechanical response of the composites, Fig. 3 displays the variation of the stress with strain for 40 mol% NiO/3YTZP and 65 mol% NiO/8YSZ at a temperature of 1300 ºC and at initial strain rate of $2x10^{-5}$ s^{-1} in air. The corresponding steady-state flow stresses for monolithic constituents are also displayed. It can be seen that the overall mechanical response of the composites is mainly related to the mechanical behavior of the softer phase because of its interconnection within the composite, acting as short-circuit for deformation. No effect of the oxygen partial pressure on the creep strength was found in oxidizing atmospheres, in agreement with that reported previously in NiO, 3YTZP and 8YSZ monoliths [6,10].

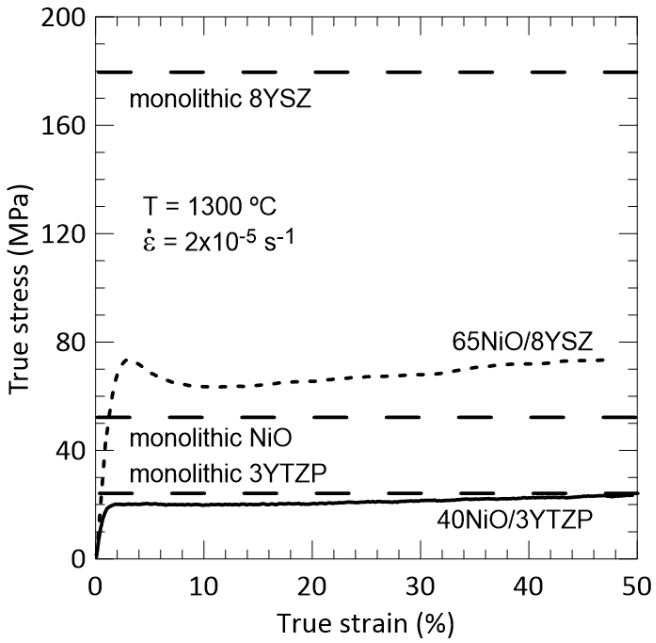

Figure 3: True stress against true strain curves for NiO/zirconia composites. Flow stresses for monolithic counterparts at the same experimental conditions are also shown.

For SOFC applications, the NiO/zirconia composite is usually reduced in situ during the first use of the device to transform the nickel oxide phase into metallic nickel. Fig. 4 compares the microstructures of the original as-fabricated NiO/8YSZ composite and after reduction in 5% H_2/95% Ar at 1200 ºC for 6 h. The reduced material shows a porous structure, with rather rounded nickel particles and pores distributed along the zirconia/nickel interfaces.

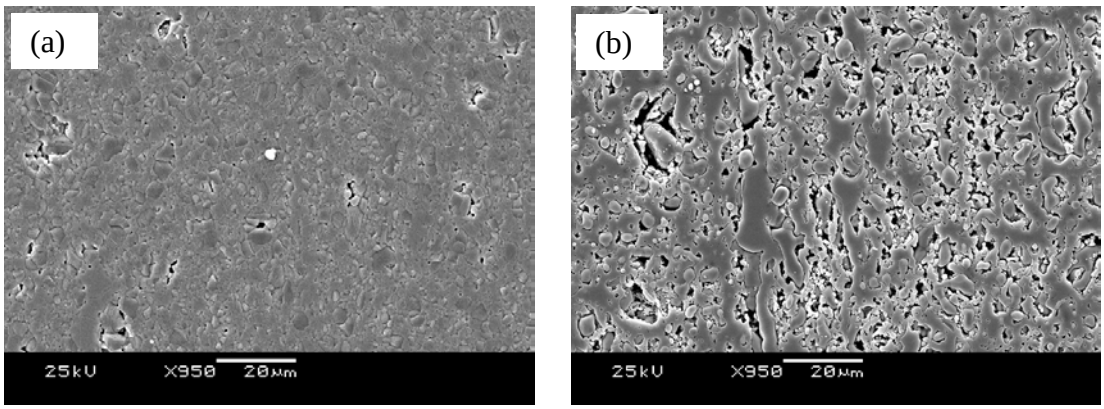

Figure 4: SEM micrographs of 65NiO/8YSZ composite: (a) as-fabricated; and (b) after treatment in reducing atmosphere (5% H_2/95% Ar, 1200 ºC, 6 h).

These microstructural changes leads to drastic changes in the mechanical behavior of the composites. Fig. 5 displays the true stress vs true strain curves for 40 mol% NiO/3YTZP composites showing jumps from air to reducing atmosphere (solid line) and vice versa (dashed line). In both cases, the samples were unloaded at each change of atmosphere for 90 min before resuming tests. It can be seen that the flow stress decreases more than three times when passing from air to hydrogen atmosphere. By contrast, there is an increase in the stress level when passing from reducing to air atmosphere. However, in this latter case, the stress level in air condition is lower than that expected from the first test. These results indicate that the microstructure is not completely recovered after forward and backward redox changes, compromising the overall integrity of the composite. A similar conclusion was drawn in a study on 65 mol% NiO/8YSZ composites [12].

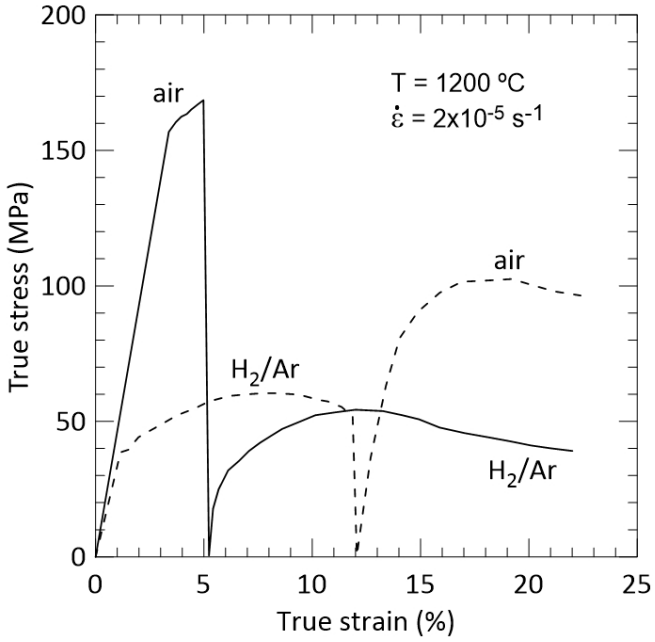

Figure 5: True stress against true strain curves for 40 mol% NiO/8YSZ composites showing atmosphere changes from air to 5% H_2/95% Ar (solid line) and vice versa (dashed line).

4 CONCLUSIONS

NiO/8YSZ and NiO/3YTZP composites with different NiO contents have been fabricated by mechanical mixing of nickel oxide and zirconia powders and sintering at 1500 ºC for 10 h in air. The compounds are highly dense, with duplex microstructures formed by NiO particles distributed throughout the zirconia matrix. Monolithic counterparts were also processed for the sake of comparison. The mechanical behaviour of the composites has been characterized by compressive constant strain rate tests at high temperatures between 1100 and 1350 ºC. The overall mechanical response of the composites is mainly related to the mechanical behavior of the softer phase because of its interconnection within the composite, acting as short-circuit for deformation. The flow stress decreases strongly in reducing atmospheres with respect to air, and vice versa. However, the increase in stress in the latter case is more moderate without attaining the original level.

ACKNOWLEDGEMENTS

This work was supported by the Project nº MAT2013-41233-R, Ministerio de Economía y Competitividad, España.

REFERENCES

[1] S.C. Singhal and K. Kendall, *High Temperature Solid Oxide Fuel Cell. Fundamentals, Design*

and Applications, Elsevier, Oxford, 2003.

[2] W. Zhu and S. Deevi, A review on the status of anode materials for solid oxide fuel cells, *Material Science and Engineering*, **A362**, 2003, pp. 228-239.

[3] H.J. Cho and G.M. Choi, Effect of milling methods on performance of Ni–Y_2O_3-stabilized ZrO_2 anode for solid oxide fuel cell, *Journal of Power Sources*, **176**, 2008, pp. 96-101.

[4] S.P. Jiang, P.J. Callus and S.P.S. Badwal, Fabrication and performance of Ni/3 mol% Y_2O_3–ZrO_2 cermet anodes for solid oxide fuel cells, *Solid State Ionics*, **132**, 2000, pp. 1-14.

[5] J.P. Poirier, *Creep of Crystals*, Cambridge University Press, Cambridge, 1985.

[6] M. Jiménez-Melendo, A. Domínguez-Rodríguez and A. Bravo-León, Superplastic Flow of Fine-Grained Yttria-Stabilized Zirconia Polycrystals: Constitutive Equation and Deformation Mechanisms, *Journal of the American Ceramic Society*, **81**, 1998, pp. 2761-2776.

[7] T.G. Nieh, J. Wadsworth and O.D. Sherby, *Superplasticity in metals and ceramics*, Cambridge University Press, Cambridge, 1997.

[8] S.K. Kurtz and F.M.A. Carpay, Microstructure and normal grain growth in metals and ceramics. Part I. Theory, *Journal of Applied Physics*, **51**, 1980, pp. 5725-5744.

[9] B. Sudhir and A.H. Chokshi, Compression Creep Characteristics of 8-mol%-Yttria-Stabilized Cubic-Zirconia, *Journal of the American Ceramic Society*, **84**, 2001, pp. 2625-2632.

[10] M. Jiménez-Melendo, A. Domínguez-Rodríguez, R. Márquez and J. Castaing, Diffusional and dislocation creep of NiO polycrystals, *Philosophical Magazine A*, **56**, 1987, pp. 767-781.

[11] J. Wolfenstine, C.D. Sperry, K.C. Goretta, J.L. Routbort, M.T. Lanagan, I. Bloom, T.D. Kaun and M. Krumpelt, Elevated-temperature creep strength of $LiFeO_2$, $LiCoO_2$ and NiO-5(at.%)Li_2O, *Materials Letters*, **31**, 1997, pp. 251-254.

[12] M. Jiménez-Melendo and F.A. Huamán-Mamani, Creep strength of nickel oxide/zirconia composites under different environmental atmospheres, *Solid State Ionics*, **225**, 2012, pp. 471-75.